Nanoparticle Synthesis

DOI: 10.1002/anie.201305289

Ammonia-in-Oil-Microemulsions and Their Application**

*Fabian Gyger, Pascal Bockstaller, Dagmar Gerthsen, and Claus Feldmann**

Dedicated to Professor Werner Uhl on the occasion of his 60th birthday

Microemulsion techniques belong to the most widely applied strategies for preparing high-quality nanoparticles, with about 1000 publications appearing each year.[1] In general, a microemulsion is a thermodynamically stable system containing surfactant-stabilized droplets that can be used as nanoreactors. They allow for a wide variability in terms of composition (for example, metals, oxides, sulfides, halides), size (typically 1–50 nm), and shape (spheres, hollow spheres, Janus-like shapes, core–shell structures).[1,2] To obtain nanoparticles, water-in-oil (*w/o*)-microemulsions, which are also called inverse microemulsions, are most often applied with water as the polar dispersed phase and an alkane (such as hexane, octane) as the nonpolar dispersant phase.[1,2] Based on aqueous polar phases, nanoparticle synthesis is restricted, however, to compounds that are neither hydrolyzed nor oxidized by water. The use of non-aqueous solvents as the polar phase, on the contrary, is comparably rare (methanol, ethylene glycol, dimethylformamide, ionic liquids).[3] Such non-aqueous microemulsion systems can take up only small portions of the polar phase and are therefore often not suitable for the synthesis of nanoparticles. As an additional restriction, the presence of at least small amounts of water often cannot be excluded.[3] For these reasons, the use of non-aqueous microemulsions for nanoparticle synthesis is limited to date.[4]

Liquid ammonia is well-known as a water-comparable solvent and it is widely used for preparing reactive bulk compounds (including less-noble metals, clusters, Zintl compounds, metal nitrides) and for particular biomolecular reactions.[5] The availability of liquid ammonia as the polar phase of a liquid-ammonia-in-oil-microemulsion could thus open the door to reactive nanomaterials under water-free conditions and under redox conditions that are otherwise hard to realize. Herein, we present the first liquid-ammonia-in-oil-microemulsion (designated as *a/o*-microemulsion). We describe how to establish such an *a/o*-microemulsion, and we demonstrate its usability based on four examples, namely Bi^0, Re^0, CoN, GaN, thus indicating the potential of the strategy regarding nanoscaled reactive metals and metal nitrides.

To establish a microemulsion with liquid ammonia as the polar phase, *n*-heptane was chosen as the continuous oil phase. Heptane is immiscible with liquid ammonia and exhibits a freezing point (−91 °C) that is well below the boiling point of liquid ammonia (−33 °C) (Figure 1). Moreover, we selected suitable amphiphiles following the concepts of the hydrophilic–lipophilic balance (HLB), the mixed-film theory, and the solubilization theory, as recently reviewed by Paul and Moulik.[6] Accordingly, a mixed film has to be established by combining suitable surfactants and cosurfactants that are of limited solubility in both hydrophilic liquid ammonia and hydrophobic heptane. First, we tested conventional monotailed quaternary ammonium salts such as cetyltrimethylammonium bromide (CTAB). These surfactants turned out as reasonably inert, but none of them matched with the HLB. Therefore, the emulsification with liquid ammonia was insufficient, and the systems remained turbid and showed phase separation.

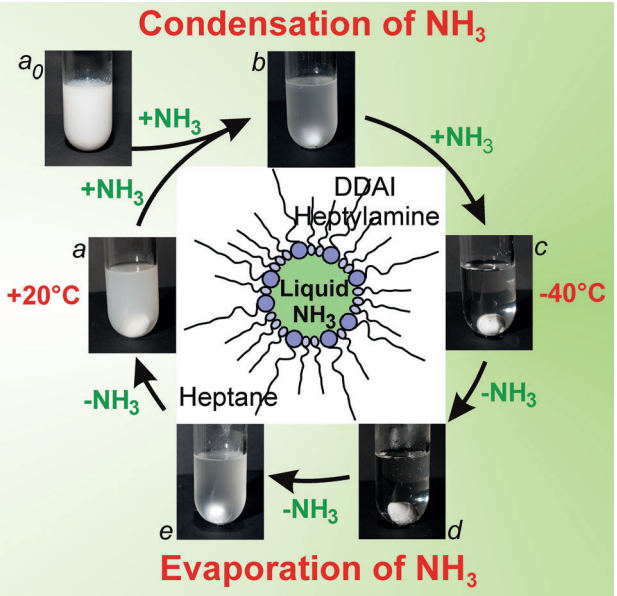

Figure 1. The microemulsion system heptane/DDAI/heptylamine upon condensation of NH_3 (a–c) and evaporation of NH_3 (c–e); (a_0) shows the virgin system prior to the first condensation of NH_3 at room temperature; c) shows the stable, fully transparent liquid-ammonia-in-oil (*a/o*)-microemulsion at −40 °C.

[*] Dr. F. Gyger, Prof. Dr. C. Feldmann
Institut für Anorganische Chemie
Karlsruhe Institute of Technology (KIT)
Engesserstrasse 15, 76131 Karlsruhe (Germany)
E-mail: claus.feldmann@kit.edu

Dipl.-Phys. P. Bockstaller, Prof. Dr. D. Gerthsen
Laboratorium für Elektronenmikroskopie
Karlsruhe Institute of Technology (KIT)
Engesserstrasse 7, 76131 Karlsruhe (Germany)

[**] The authors are grateful to the Deutsche Forschungsgemeinschaft (DFG) for individual grants as well as to the DFG-Center of Functional Nanostructures (CFN) at the KIT for instrumental support.

Supporting information for this article is available on the WWW under http://dx.doi.org/10.1002/anie.201305289.

To enhance the lipophilic character of the surfactant tail and to favor the formation of a microemulsion, doubletailed surfactants were tested next. Thus, an emulsification of liquid ammonia and *n*-heptane was achieved with dimethyldioctylammonium bromide or iodide (DDAB, DDAI) as cationic surfactant, and resulted in a turbid macroemulsion. Notably, both surfactants, DDAB and DDAI, are hardly soluble in both liquid ammonia and heptane. In accordance with mixed-film theory, the charge density of the cationic surfactant now has to be moderated by addition of a non-charged cosurfactant. Here, hexylamine or heptylamine have been selected. The resulting *a/o*-microemulsion is shown in Figure 1. Most importantly, clarification of the *a/o*-microemulsion was only observed for the selected surfactant/cosurfactant system and only after condensation of liquid ammonia (0.1–0.5 mL; see the Supporting Information). The occurrence of a fully transparent system in the presence of liquid ammonia and the turbidity of the system when evaporating liquid ammonia turned out to be highly reversible (Figure 1). Although indirect, this reversible clarification is a characteristic feature that indicates the presence of a thermodynamically stable *a/o*-microemulsion.

For conventional water-based microemulsions, Pileni pointed out that the size of the water pool is a decisive difference between a micellar solution and a microemulsion.[7] With ionic surfactants, a microemulsion is only established for water-to-surfactant ratios of $\omega_{H_2O} \geq 15$ ($\omega_{H_2O} = [H_2O]/[\text{surfactant}]$). Only then the number of water molecules exceeds the number of molecules needed to hydrate the charged surfactant-heads and their counterions. Or in other words, only with $\omega_{H_2O} \geq 15$ "free" water and an aqueous pool for performing reactions is present in the microemulsion.[8] For the *a/o*-microemulsion established here, ammonia-to-surfactant ratios (ω_{NH_3}) up to $\omega_{NH_3} = 22$ ($\omega_{NH_3} = [NH_3]/[\text{surfactant}]$) were obtained that strongly suggest the presence of "free" ammonia molecules, and therefore legitimates the description as a liquid-ammonia-in-oil-microemulsion (Supporting Information, Table S1). Additional features indicate the characteristic behavior of a microemulsion as well. For example, the maximum uptake of liquid ammonia in the system also correlates with the surfactant-to-cosurfactant ratio (Supporting Information, Table S1).[6] Another characteristic feature of an inverse microemulsion is the possibility to dissolve metal salts inside the polar droplets. Here, $KMnO_4$ has been selected as an illustrative example of an ionic compound that can be easily detected by the naked eye owing to its deep red color. The obtained homogenous liquid phase with "free" ammonia being the only component to solubilize $KMnO_4$, again points to the presence of an *a/o*-microemulsion (Supporting Information, Figure S1).

As the next step, we studied the usability of our *a/o*-microemulsion for the synthesis of nanoparticles. As a first case study, we present Bi^0, Re^0, CoN and GaN. As Bi^0 nanoparticles have been already prepared in water-based microemulsions,[9] the synthesis of Bi^0 nanoparticles in the *a/o*-microemulsion was selected as a starting point of our case study. Subsequent to synthesis and careful washing, the as-prepared Bi^0 nanoparticles were obtained as a fine black powder that can be easily redispersed in chloroform. Overview-TEM and HRTEM images show spherical nanoparticles with a mean diameter of 6.6 ± 1.2 nm (Figure 2; Supporting Information, Figures S3, S5). The observed lattice fringes (3.2 Å) indicate the crystallinity and composition of single nanoparticles (Bi^0: [012] with 3.28 Å). Composition and crystallinity of a statistically relevant number of the as-prepared nanoparticles are further confirmed by X-ray powder diffraction (XRD) and selected-area electron diffraction (SAED; Figure 2). The obtained lattice parameters (XRD: $a = 4.52$, $c = 11.92$ Å; SAED: $a = 4.53$, $c = 11.88$ Å) are well in accordance with rhombohedral bismuth ($a = 4.55$, $c = 11.86$ Å). The broadening and reduced intensity of the Bragg peaks can be ascribed to size and strain of the nanoparticles. Energy-dispersive X-ray spectroscopy (EDXS) and FTIR spectroscopy also validate the composition of the as-prepared Bi^0 nanoparticles (Supporting Information, Figures S4, S6).

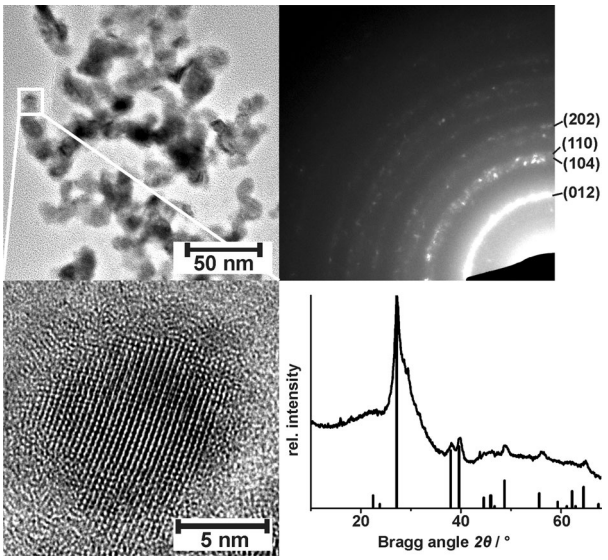

Figure 2. TEM, HRTEM, SAED, and XRD of as-prepared Bi^0 nanoparticles from *a/o*-microemulsions (reference: Bi/ICCD-No. 44-1246).

As the Bi^0 nanoparticles corroborate the principal usability of the *a/o*-microemulsion, we next aimed at Re^0 nanoparticles as a more ambitious example. Interestingly, reports on the synthesis of nanoscaled Re^0 are rare to date. They include the reduction of K_2ReCl_6 or $KReO_4$ with hydrazine or cyclic triphosphazenes.[10] Moreover, Re^0 nanoparticles were obtained by thermal decomposition of $[Re_2(CO)_{10}]$ in ionic liquids.[11] In view of the extraordinary catalytic activity of Re^0 nanoparticles (for example, Fischer–Tropsch process, hydrogenolysis, electrocatalysis),[12] this limited accessibility is surprising but can be ascribed to its high reactivity. Using *a/o*-microemulsions, we have obtained partially facetted Re^0 nanoparticles with a mean diameter of 2.2 ± 0.3 nm (Figure 3; Supporting Information, Figures S2, S3, S7). A Fourier transformation of the lattice spacing observed on HRTEM images (2.1 and 2.2 Å) clearly points to hexagonal rhenium ((101) with 2.11 Å; (002) with 2.23 Å; Figure 3). After sintering, the obtained Bragg peaks clearly confirm the phase purity that is also validated by EDXS and FTIR spectroscopy for the as-prepared Re^0 nanoparticles (Figure 3; Supporting Informa-

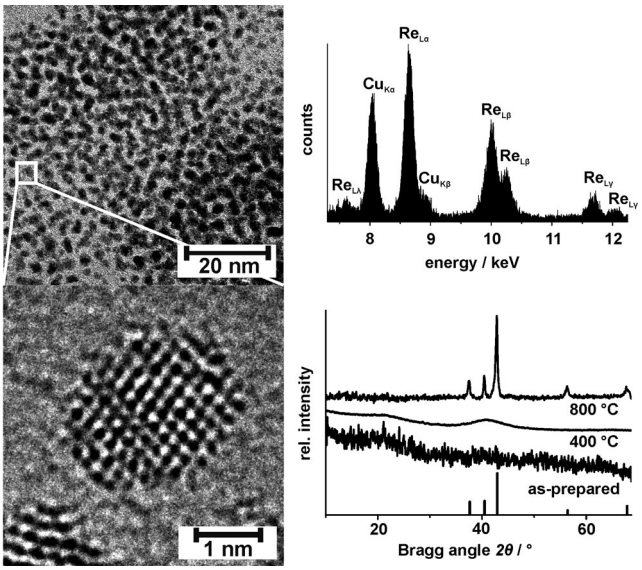

Figure 3. TEM, HRTEM, EDXS (on copper grid), XRD of as-prepared Re^0 nanoparticles from *a/o*-microemulsions, and XRD of sintered particles (400 °C, 800 °C; reference: Re/ICCD-No. 5-702).

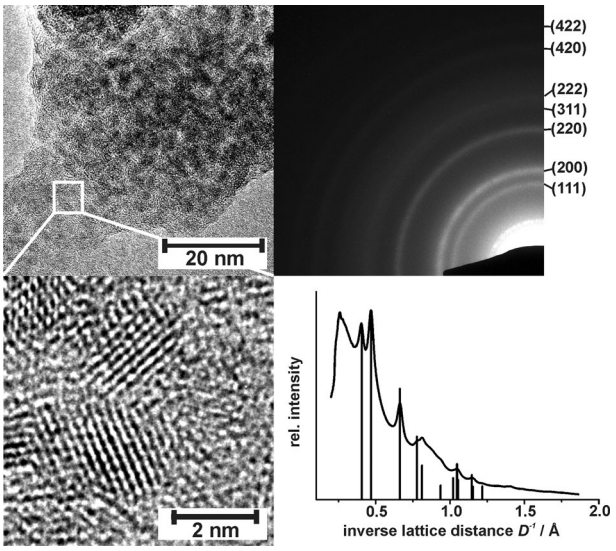

Figure 4. TEM, HRTEM, SAED, and diffraction pattern (intensity deduced from SAED plotted against inverse lattice distance) of as-prepared CoN nanoparticles from *a/o*-microemulsions (reference: CoN with NaCl-type structure: $a = 4.27$ Å).[17]

tion, Figures S4, S8). Thus, only rhenium is detected by EDXS, whereas oxygen impurities turned out to be negligible.

With regard to metal nitrides, the direct ammonolysis of metal compounds is typically hampered by the low acidity of the amide (NH_2^-) and imide (NH^{2-}) intermediates.[13] Thus, high-temperature sintering (≥ 200 °C) is needed for complete ammonolysis and formation of crystalline metal nitrides. For nanoparticles, such sintering is detrimental owing to severe particle agglomeration. If oxides are used for ammonolysis, oxygen impurities can hardly be avoided. These limitations motivated us to exemplarily try the synthesis of CoN and GaN in *a/o*-microemulsions. Nanoscaled CoN is yet only available by high-temperature ammonolysis (≥ 300 °C) of $NiCo_2O_4$, Co_3O_4, or $Co(NH_3)_6(NO_3)_3$.[14] High-quality CoN nanoparticles, on the other hand, are highly sought-after as they are very promising for high-capacity anodes in lithium-ion batteries or as a high-activity catalyst for hydrodenitrogenation, NO decomposition, and solid-oxide fuel cells.[14,15] Nanoscaled GaN as a wide-band-gap semiconductor (3.3–3.5 eV) is discussed intensely for its quantum-confinement effects as well as for optoelectronic applications.[13] Nanocrystalline GaN powders were obtained by nitridation of the metal, ammonolysis of oxides, and thermal decomposition of molecular, nitrogen-rich precursors.[13,16] Referring to this, further improvement in view of oxygen- and defect-free, non-sintered, and non-agglomerated GaN nanoparticles of controlled size and surface-conditioning was discussed.[13a,b]

The formation of CoN nanoparticles in the *a/o*-microemulsion can be followed by the naked eye (Supporting Information, Figure S9). Thus, the color change from blue $Co(NH_2)_2$ to black CoN indicates the proceeding ammonolysis. The resulting CoN exhibits a uniform spherical shape and a mean diameter of 2.3 ± 0.3 nm (Figure 4; Supporting Information, Figures S3, S10). The observed lattice fringes (2.1 Å) indicate the crystallinity of the as-prepared nanoparticles and a NaCl-type structure (CoN_{NaCl}: (200) with 2.14 Å).[17] This finding is confirmed by SAED (Figure 4). Here, all of the reflections can be indexed based on NaCl-type CoN with a lattice parameter of 4.26 Å (CoN_{NaCl}: $a =$ 4.27 Å).[17] Considering the fact that certain sintering ($\geq$ 300 °C) is needed to crystallize CoN,[13–15] the realization of crystalline CoN right from the *a/o*-microemulsion is surprising. The composition of the CoN nanoparticles is further indicated by FTIR spectroscopy and EDXS (Supporting Information, Figures S4, S11, Table S2). The Co:N ratio can be indeed deduced to 1.0:1.1.

GaN nanoparticles obtained from the *a/o*-microemulsion exhibit a mean diameter of 3.2 ± 0.5 nm (Figure 5; Supporting Information, Figures S3, S12). Similar to CoN, HRTEM images show crystalline particles although the synthesis was performed at −40 °C. The observed lattice spacing of 2.6 Å matches with sphalerite-type β-GaN (β-GaN: (111) with 2.60 Å).[18] The composition of the as-prepared GaN is confirmed by FTIR spectra confirming the absence of any significant N–H or O–H vibrations, but showing a broad absorption at 600 cm^{-1} as it was postulated for crystalline GaN (Supporting Information, Figure S4).[19] EDXS confirms a Ga:N ratio of 1.0:1.0 (Supporting Information, Figure S13, Table S3). XRD shows the characteristic Bragg peaks of β-GaN as broad reflections (Figure 5). After sintering, the characteristic Bragg peaks become sharper. At 800 °C the strongest Bragg peak still indicates the presence of cubic β-GaN, along with the reflections of wurzite-type α-GaN now present. The crystallinity of the as-prepared β-GaN nanoparticles is finally shown by photoluminescence (PL) spectroscopy. Despite the preparation at −40 °C, the characteristic excitation ($\lambda_{max} = 290$ nm) and emission ($\lambda_{max} = 336$ nm) are clearly visible (Figure 5). In comparison to bulk-β-GaN,[13,16] the excitation is blue-shifted by about 1 eV, as is to be expected in view of the particle size and quantum-confine-

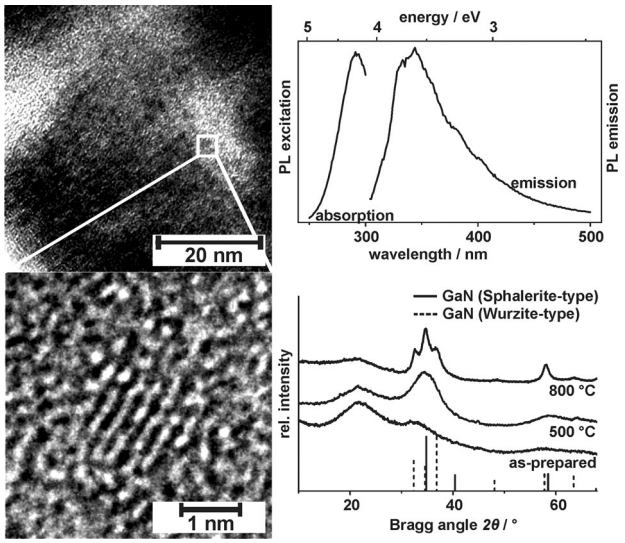

Figure 5. TEM, HRTEM, PL, and XRD of as-prepared β-GaN nanoparticles from *a/o*-microemulsions, and XRD of sintered particles (500 °C, 800 °C; references: β-GaN/sphalerite-type/ICCD-No. 1088-2364, α-GaN/wurzite-type/ICCD-No. 50-792).

ment of the β-GaN nanoparticles. Although synthesized at −40 °C to +25 °C, the absorption and emission band are similar or even more narrow than reported for GaN nanoparticles treated at temperatures of ≥200 °C.[13,16] This indicates a similar or even lower defect concentration (for example, lattice defects, oxide antisites) of the as-prepared β-GaN. The formation of crystalline CoN and GaN can thus be ascribed to the high molar concentration of NH_3 and the absence of water in liquid ammonia.

In conclusion, a liquid-ammonia-in-oil-(*a/o*)-microemulsion is presented for the first time. With heptane as the polar phase, DDAB/DDAI as cationic surfactant, and hexyl-/heptylamine as the cosurfactant, a thermodynamically stable microemulsion is reproducibly obtained and can be handled as easily as a standard *w/o*-microemulsion (apart from the lower temperature of −40 °C needed for liquid ammonia). As a case study, the synthesis of Bi^0, Re^0, CoN, and GaN nanoparticles exhibiting a mean diameter in the 1–8 nm range is shown. Surprisingly, crystalline nanoparticles can be readily obtained without any additional thermal treatment. Based on the unique solvent properties of liquid ammonia, in sum, nanomaterials that are highly sensitive towards hydrolysis and/or oxidation are accessible. The *a/o*-microemulsion established here can open the door to many more reactive nanomaterials (for example, less-noble metals, Zintl phases, metal nitrides) and allows study of their fundamental properties (such as quantum-confinement effects) and their potential application (for example, catalysis, high-power batteries, solar cells).

Experimental Section

Liquid-ammonia-in-oil (a/o) microemulsion: The liquid ammonia-in-oil (*a/o*) microemulsion was established by dissolving dimethyldioctylammonium iodide (DDAI; 0.50 g, 1.25 mmol; see the Supporting Information for synthesis) as the surfactant and heptylamine (3.34 g, 22.5 mmol) as the cosurfactant in heptane (15 mL) as the non-polar oil-phase. Subsequently, the resulting turbid emulsion was cooled to −40 °C and ammonia (0.5 mL) was condensed whereupon clarification occurred and the *a/o*-microemulsion was formed. Further details regarding synthesis and analytical characterization can be found in the Supporting Information.

Bi^0 nanoparticles were prepared by first dissolving $NaBH_4$ (8.3 mg, 0.22 mmol). After the addition of this first starting material, the *a/o*-microemulsion remained fully transparent. Next, BiI_3 (41.7 mg (0.07 mmol) was added. Upon adding BiI_3, the microemulsion turned to deep black after few minutes. After 30 min, NH_3 was allowed to evaporate by natural warming to room temperature. The *a/o*-microemulsion was destabilized by adding acetonitrile (15 mL). Thereafter, the nanoparticles were separated by centrifugation and washed three times by redispersion/centrifugation in/from chloroform.

Re^0 nanoparticles were prepared similarly to the Bi^0 nanoparticles. Thus, $NaBH_4$ (11 mg, 0.29 mmol) was first dissolved in the *a/o*-microemulsion. Next, ReI_3 (44 mg, 0.078 mmol) was added. The colorless *a/o*-microemulsion instantaneously turned black, indicating the formation of Re^0. After destabilization, the as-prepared Re^0 was purified once by redispersion/centrifugation in/from a 1:1 mixture of chloroform and acetonitrile, followed by redispersing/centrifugating three times in/from pure chloroform.

CoN nanoparticles were prepared by sequential addition of freshly prepared KNH_2 (36.7 mg, 0.67 mmol; see the Supporting Information) and CoI_2 (105 mg, 0.34 mmol) to the *a/o*-microemulsion. After the addition of CoI_2, the *a/o*-microemulsion first turned opalescent and then slowly became blue, indicating the formation of cobalt amide $Co(NH_2)_2$ (Supporting Information, Figure S9). After 1 h, the suspension was allowed to warm to room temperature to evaporate NH_3. Subsequently, the suspension was heated to refluxing heptane (98 °C). Within 1 h, the suspension became deep black under gas evolution (Supporting Information). After destabilization, the as-prepared CoN was purified once by redispersion/centrifugation in/from acetonitrile, followed by redispersion/centrifugation three times in/from ethanol. Ethanol as a polar solvent was necessary to remove excess KNH_2.

GaN nanoparticles were prepared by dissolving NH_4I (46.2 mg, 0.32 mmol) in the *a/o*-microemulsion, followed by the addition of freshly prepared $NaGa(NH_2)_4$ (50 mg, 0.32 mmol; synthesis according to Ref. [20]). After 30 min, the *a/o*-microemulsion was allowed to warm to room temperature. After destabilization, the as-prepared GaN was purified once by redispersion/centrifugation in/from acetonitrile, followed by redispersion/centrifugation three times in/from ethanol. Ethanol as a polar solvent was necessary to remove non-reacted $NaGa(NH_2)_4$.

Received: June 19, 2013
Revised: August 5, 2013
Published online: September 25, 2013

Keywords: liquid ammonia · metals · metal nitrides · microemulsions · nanoparticles

[1] a) A. K. Ganguli, A. Ganguly, S. Vaidya, *Chem. Soc. Rev.* **2010**, *39*, 474; b) S. P. Moulik, A. K. Rakshit, I. Capek in *Microemulsions* (Ed.: C. Stubenrauch), Wiley-VCH, Weinheim, **2009**, p. 180; c) M. P. Pileni, *Nat. Mater.* **2003**, *2*, 145.

[2] a) H. Goesmann, C. Feldmann, *Angew. Chem.* **2010**, *122*, 1402; *Angew. Chem. Int. Ed.* **2010**, *49*, 1362; b) J. Eastoe, M. J. Hollamby, L. Hudson, *Adv. Colloid Interface Sci.* **2006**, *128*, 5; c) Y. N. Xia, J. A. Rogers, K. E. Paul, G. M. Whitesides, *Chem. Rev.* **1999**, *99*, 1823.

[3] a) N. M. Correa, J. J. Silber, R. E. Ritter, N. E. Levinger, *Chem. Rev.* **2012**, *112*, 4569; b) W. Kunz, T. Zemb, A. Harrar, *Curr. Opin. Colloid Interface Sci.* **2012**, *17*, 205; c) F. Gao, C. C. Co in *Microemulsions* (Ed.: C. Stubenrauch), Wiley-VCH, Weinheim, **2009**, p. 211.

[4] a) D. Tanaka, A. Henke, K. Albrecht, M. Möller, K. Nakagawa, S. Kitagawa, J. Groll, *Nat. Chem.* **2010**, *2*, 410; b) P. Setua, R. Pramanik, S. Sarkar, C. Ghatak, S. K. Das, N. Sarkar, *J. Phys. Chem. B* **2010**, *114*, 7557; c) P. Setua, A. Chakraborty, D. Seth, M. U. Bhatta, P. V. Satyam, N. Sarkar, *J. Phys. Chem. C* **2007**, *111*, 3901; d) G. N. Karanikolos, P. Alexandridis, G. Itskos, A. Petrou, T. J. Mountziaris, *Langmuir* **2004**, *20*, 550; e) V. Chhabra, M. Lal, A. N. Maitra, P. Ayyub, *J. Mater. Res.* **1995**, *10*, 2689.

[5] a) S. Scharfe, F. Kraus, S. Stegmaier, A. Schier, T. F. Fässler, *Angew. Chem.* **2011**, *123*, 3712; *Angew. Chem. Int. Ed.* **2011**, *50*, 3630; b) J. J. Lagowski, *Synth. React. Inorg. Met.-Org. Nano-Met. Chem.* **2007**, *37*, 115; c) P. Ji, J. Atherthon, M. I. Page, *Org. Biomol. Chem.* **2012**, *10*, 5732.

[6] B. K. Paul, S. P. Moulik, *J. Dispersion Sci. Technol.* **1997**, *18*, 301.

[7] M. P. Pileni, *J. Phys. Chem.* **1993**, *97*, 6961.

[8] A. Maitra, *J. Phys. Chem.* **1984**, *88*, 5122.

[9] a) R. J. de Olivera, P. Brown, G. B. Correia, S. E. Rogers, R. Heenan, I. Grillo, A. Galembeck, J. Eastoe, *Langmuir* **2011**, *27*, 9277; b) C. Stubenrauch, T. Wielpuetz, T. Sottmann, C. Roychowdhury, F. C. Di Salvo, *Colloids Surf. A* **2008**, *317*, 328; c) L. Balan, R. Schneider, D. Billaud, Y. Fort, J. Ghanbaja, *Nanotechnology* **2004**, *15*, 940; d) E. E. Foos, R. M. Stroud, A. D. Berry, A. W. Snow, J. P. Armistead, *J. Am. Chem. Soc.* **2000**, *122*, 7114.

[10] a) C. D. Valenzuela, M. L. Valenzuela, S. Caceres, C. O'Dywer, *J. Mater. Chem. A* **2013**, *1*, 1566; b) M. R. Mucalo, C. R. Bullen, *J. Colloid Interface Sci.* **2001**, *239*, 71.

[11] a) Y. Y. Chong, W. Y. Chow, W. Y. Fan, *J. Colloid Interface Sci.* **2012**, *369*, 164; b) C. Vollmer, E. Redel, K. Abu-Shandi, R. Thomann, H. Manyar, C. Hardacre, C. Janiak, *Chem. Eur. J.* **2010**, *16*, 3849; c) G. H. Lee, S. H. Huh, S. H. Kim, B. J. Choi, *J. Korean Phys. Soc.* **2003**, *42*, 835.

[12] a) U. G. Hong, H. W. Park, J. Lee, S. Y. Hwang, J. Yi, I. K. Song, *Appl. Catal. A* **2012**, *415–416*, 141; b) M. Chia, Y. J. Pagan-Torres, D. Hibbitts, Q. H. Tan, H. N. Pham, A. K. Datye, M. Neurock, R. J. Davis, J. A. Dumesic, *J. Am. Chem. Soc.* **2011**, *133*, 12675; c) R. R. Soares, D. A. Simonetti, J. A. Dumesic, *Angew. Chem.* **2006**, *118*, 4086; *Angew. Chem. Int. Ed.* **2006**, *45*, 3982; d) J. Zhang, M. B. Vukmirovic, K. Sasaki, A. U. Nilekar, M. Mavrikakis, R. R. Adzic, *J. Am. Chem. Soc.* **2005**, *127*, 12480; e) J. Greeley, M. Mavrikakis, *Nat. Mater.* **2004**, *3*, 810.

[13] a) L. Xu, S. Li, Y. Zhang, Y. Zhai, *Nanoscale* **2012**, *4*, 4900; b) C. Giordano, M. Antonietti, *Nano Today* **2011**, *6*, 366; c) E. Horvath-Bordon, R. Riedel, A. Zerr, P. F. McMillan, G. Auffermann, Y. Prots, W. Bronger, R. Kniep, P. Kroll, *Chem. Soc. Rev.* **2006**, *35*, 987.

[14] a) B. Das, M. V. Reddy, B. V. R. Chowdari, *Nanoscale* **2013**, *5*, 1961; b) R. S. Ningthoujam, R. N. Panda, N. S. Gajbhiye, *Mater. Chem. Phys.* **2012**, *134*, 377; c) Y. Shi, R. Zhang, D. Zhao, *Adv. Funct. Mater.* **2008**, *18*, 2436.

[15] a) V. Mazumder, Y. Lee, S. Sun, *Adv. Funct. Mater.* **2010**, *20*, 1224; b) Z. Yao, A. Zhu, C. Shi, *Catal. Lett.* **2009**, *130*, 63.

[16] a) B. Schwenzer, J. Hu, D. E. Morse, *Adv. Mater.* **2011**, *23*, 2278; b) Y. Chen, N. Jyoti, J. Kim, *Appl. Phys. A* **2011**, *102*, 517; c) R. Deshmukh, U. Schubert, *J. Mater. Chem.* **2011**, *21*, 18534; d) G. Pan, M. E. Kordesch, P. G. Van Patten, *Chem. Mater.* **2006**, *18*, 3915–3917; e) A. Manz, A. Birkner, M. Kolbe, R. A. Fischer, *Adv. Mater.* **2000**, *12*, 569.

[17] O. Schmitz-Dumont, N. Kron, *Angew. Chem.* **1955**, *67*, 231.

[18] A. P. Purdy, *Chem. Mater.* **1999**, *11*, 1648.

[19] W.-S. Jung, *Mater. Lett.* **2002**, *57*, 110.

[20] H. Jacobs, B. Nöcker, *Z. Anorg. Allg. Chem.* **1993**, *619*, 381.

